

# 1 Final Technical Report

Covering the period 09/01/1997 to 11/30/2011

## Development and Applications of Photosensitive Device Systems to Studies of Biological and Organic Materials

Grant DE-FG02-97ER62443

P.I.: Sol M. Gruner  
Department of Physics  
Cornell University

29 January 2012

### 1.1 Overview

The primary focus of the grant is the development of new x-ray detectors for biological and materials work at synchrotron sources, especially Pixel Array Detectors (PADs), and the training of students via research applications to problems in biophysics and materials science using novel x-ray methods. By any measure, the work of this grant has been extremely successful, resulting in technology that has had world-wide impact and roughly 250 papers, abstracts and reports. Details about these accomplishments have been given in the annual progress reports and the 3-year renewal proposals. This Final Progress Report will, therefore, be restricted to a high-level overview of the most important accomplishments. These major areas of accomplishment include:

- (1) Development and application of x-ray Pixel Array Detectors.
- (2) Development and application of methods of high pressure x-ray crystallography as applied to proteins.
- (3) Studies on the synthesis and structure of novel mesophase materials derived from block co-polymers.

Note that this grant was a logical and seamless continuation of an earlier DOE-BER grant to the P.I. when he was at Princeton University. The grant being reported on below commenced when the P.I. moved to Cornell University in 1997. The earlier grant period also had numerous major accomplishments which will not be described below. However, if a single most significant item had to be chosen from that grant period it would be the development of much of the CCD detector technology that now dominates macromolecular data collection at synchrotron x-ray sources [1, 2]. It is fair to say that a majority fraction of the entries of macromolecular structure in the protein data bank resulted from data collected on CCD detectors, much of the technology of which was accomplished under the prior grant. Other significant accomplishments of the prior grant period, which have continued into the 1997 – 2011 period, were seminal x-ray studies of

biomembranes [3-5], development of technology to study macromolecular systems under high pressure [6], and elucidation of bicontinuous mesophase materials derived from block co-polymers [7].

## **1.2 Pixel Array Detectors (PADs)**

### **1.2.1 PAD Development Introduction**

The need for better x-ray detectors has been repeatedly emphasized by the synchrotron radiation community as necessary to improve utilization of synchrotron radiation (SR) resources [8-12]. Significantly, detectors have consistently been cited as the progress-limiting technology at existing storage ring-based synchrotron sources; detectors will be even more limiting at proposed next generation XFEL and ERL sources unless new technologies are developed. For example, exciting SR experiments that have been proposed in areas such as multiple-frame Laue protein crystallography, dynamics of muscle, liquid crystal and polymer phase transitions and dynamics, crack propagation and materials failure, x-ray speckle diffraction, laser processing of materials, photochemical surface reactions, and chemical kinetics. Even though existing SR sources often yield sufficient numbers of x-rays to perform such experiments, existing detectors lack the flexibility and speed needed to perform many of these experiments. This situation will only get worse with next generation sources.

The approach taken under this grant has been to develop programmable silicon-based area PADs in which reconfigurable data processing hardware is integral to the detector. The detectors consist of a two-dimensional arrays of radiation-sensitive pixels fabricated on monolithic silicon wafers bump-bonded to custom designed CMOS Application Specific Integrated Circuits (ASICs). Each pixel has its own electronic cell on the ASIC, consisting of photon counting and signal conditioning electronics. As detailed, below, this uniquely powerful and flexible design enables x-ray experiments which are unfeasible with any other existing detector technology.

PADs are the quantitative imaging x-ray technology of the future. PADs are slowly displacing the CCD x-ray detectors that are the most prevalent x-ray imagers at SR and home sources today. PADs come in two variants: (1) photon counters in which each x-ray is detected and added to in-pixel digital memory and (2) analog integrators in which the x-ray signal is summed in analog fashion in the pixel prior to digitization. Each of these variants has unique strengths for specific applications.

The work under this grant has focused exclusively on analog integrators that are necessary for very high instantaneous flux applications, such as at X-ray Free Electron Lasers (XFELs). However, it is noteworthy that the most successful photon counting PAD, the Swiss Light Source Pilatus PAD, was co-developed with Dr. Eric Eikenberry. Dr. Eikenberry moved to Switzerland to assist in this development and is now co-owner of the company (Dectris) that vends the resultant PAD. Dr. Eikenberry honed his detector skills during the decade when he was a member of the P.I.'s DOE-BER

supported detector group at Princeton University. This simply illustrates that the PAD development community is small, but highly international, with a great degree of cooperation and information exchange between the few groups that have been responsible for the most significant PAD developments over the last decade.

History has taught that the development of a new detector technology requires many years of dedicated attention by a team of experienced detector designers. In the case of PADs, technology based on large scale custom fabricated integrated circuits (ICs) is very expensive to develop: a single full scale IC fabrication – and several are usually required -- may cost over \$200k, far exceeding the resources that were available under this grant. Personnel costs are even higher. It is estimated that development of the Pilatus involved over 50 person-years of effort. Each of the PADs described below involves some 10 – 20 person years. For this reason, the work described below has involved additional grants. However, this DOE-BER grant was central to them all in that it provided for the long-term development of infrastructure and support of the personnel that made work under the other grants possible.

Below, we describe progress on five PADs based on support from this DOE-BER grant. The (1) Prototype Microsecond Imager involved additional support from DOE-BES; (2) the MMPAD was a collaborative project with Area Detectors Systems Corp. (Poway, CA) under an NIH-NCRR SBIR award; (3) the LCLS PAD was part of the DOE-BES supported construction of the Linac Coherent Light Source (LCLS) at SLAC; (4) the Keck PAD is being developed with a grant from the Keck Foundation; (5) and the FPGA PAD is proceeding with DOE-BES and Keck Foundation support.

#### **1.2.1.1 Prototype Microsecond Imager**

Initial work focused on development of a prototype microsecond framing PAD [13-19]. This PAD is based on analog charge integration followed by analog-to-digital conversion. The signal from each radiation-sensing pixel is successively multiplexed and integrated into the first of several capacitors associated with that pixel (Figs. 1 & 2). Externally applied signals multiplex all the pixels in the array in parallel. After suitable x-ray exposure, the signal is synchronously multiplexed into the second storage capacitor of each pixel; the process may be repeated until all the capacitors in the pixel are used. The dead time in switching from one capacitor to another is  $< 1 \mu\text{s}$ . The minimum time to completely fill a capacitor is limited by the amplifiers in each pixel to a few microseconds for 16-bit imaging and  $< 500 \text{ ns}$  for 10-bit imaging. Eight images (i.e., frames) can be successively stored in the CMOS layer before any off-PAD readout is required. The exposure time for each of the images can be varied from sub-microsecond to minutes simply by changing the timing of the multiplexing signals. To read out the stored images, the voltage stored on each capacitor is sequentially multiplexed through the output amplifier and then through a multiplexer structure on the edge of the chip (not shown in Fig. 1) for off-chip analog-to-digital conversion and storage in computer memory.

These prototype PAD chips were fabricated in 1999 (Figure 2) in a CMOS process that is no longer available. Effort since that time has been on developing a series of

microsecond SR applications [20-27]. Count-rates in some of these applications exceeded  $10^{11}$  x-rays/pix/s. Major accomplishments have included the first x-ray imaging of the Mach cone in a gas from a supersonic fuel injector jet [24] and the first x-ray movies showing the dynamics of direct chamber gasoline fuel injectors [20]. Both of these studies have been important towards understanding fuel injection in internal combustion engines. The imager was also involved in some of the first timer resolved x-ray studies of single-shot reactive metal foil phase behavior [26, 27]. These foils are important in brazing applications.

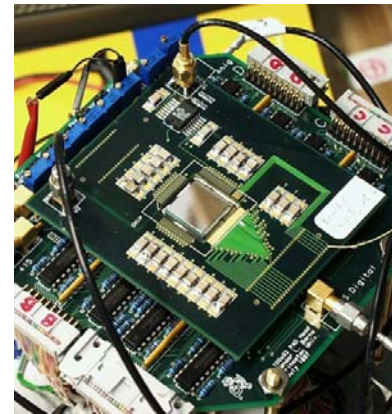
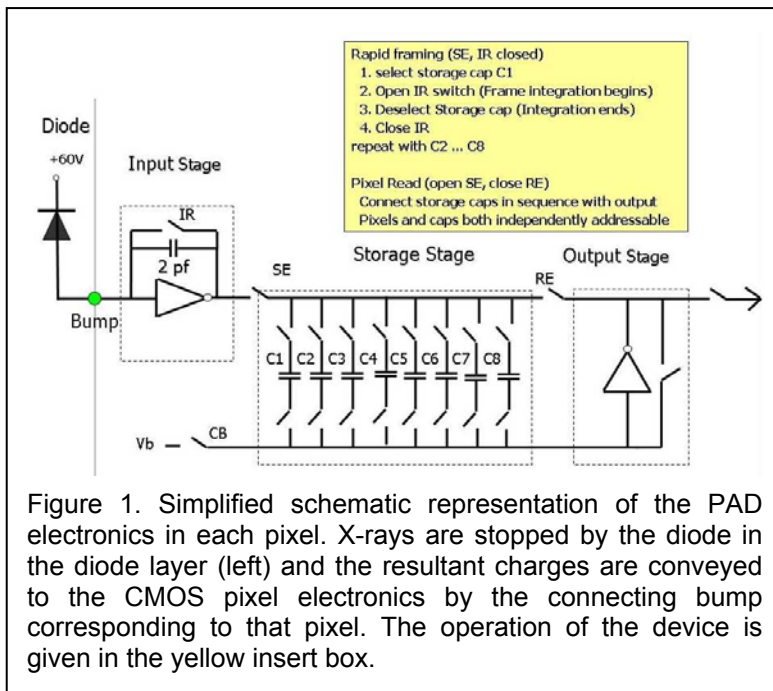


Figure 2. Prototype Microsecond PAD (silvery chip in center) is shown in a mother board of control electronics.

The success of the Prototype Microsecond Imager has led directly to the Keck PAD, described below. The capacitor storage scheme demonstrated in the Prototype Microsecond Imager is now also used in two of the three PADs being developed in Europe for the European XFEL.

### 1.2.1.2 Mixed-Mode PAD (MMPAD)

The dynamic range of the Prototype Microsecond Imager is limited to several thousand x-rays by the size of the storage capacitors. The goal of the Mixed-Mode PAD (MMPAD) was to increase the pixel dynamic range for frame rates of up to 1 KHz for advanced crystallography experiments [21, 28-30]. The development of this detector is fully described in the PhD thesis of Dan Schuette [31]. The basic scheme is shown in Fig. 3. The detector chips are capable of framing at 1 KHz with a dynamic range per pixel per frame of  $2.6 \times 10^7$  12 keV x-rays! Figure 5 shows what can be seen with such an amazing dynamic range. Figure 4 shows two types of x-ray images.

The idea behind this detector (Figure 3) is to analog integrate x-rays in fixed packets, each of which is equivalent to a selectable amount of up to  $\sim 200$  x-rays for each digital

count. The pixel architecture is schematized in Figure 3. Because x-rays are analog grouped into packets of up to 200 x-rays, very high instantaneous count rates can be accommodated, while the 18-bit in-pixel counter gives enormous dynamic range (i.e.,

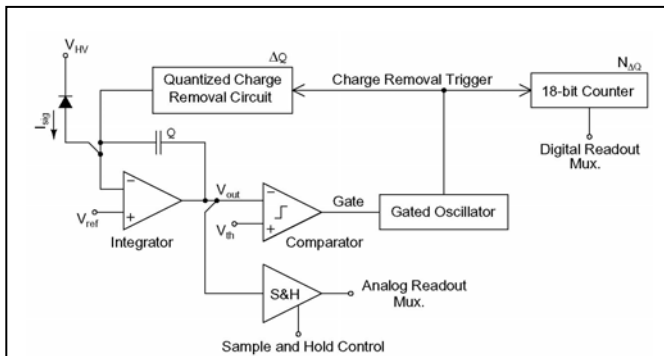


Figure 3. Simplified schematic representation of the MMPAD pixel. X-rays are stopped by the diode in the diode layer and the resultant charge is integrated. When the integrated voltage rises to a reference voltage, a digital bit is added into an 18-bit counter and a charge removal circuit is engaged to subtract a “packet” of charge from the integration capacitor. In this way, the pixel counts packets, with the number of x-rays equivalent to a packet set by the reference voltage. During readout, any remaining analog signal is sampled and routed to an ADC, for a low-order digital word; the 18-bit counter is then the high order word.

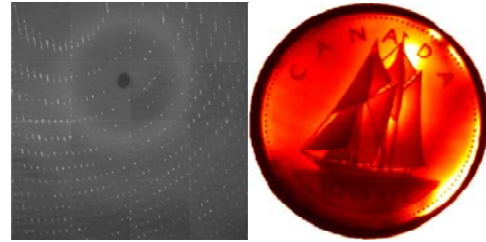


Figure 4. (Left) Uncorrected thaumatin diffraction pattern made by translating a single chip MMPAD detector stepwise over the diffraction pattern area. (Right) X-radiograph of a Canadian dime. The backside of the coin was ground away to simplify the image and allow x-ray transmission. The image is processed to reduce the appearance of pixilation (the format of the chip is 128 x 128 pixels).

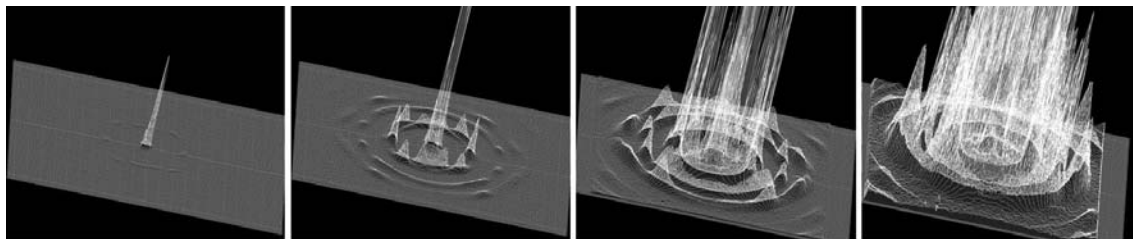


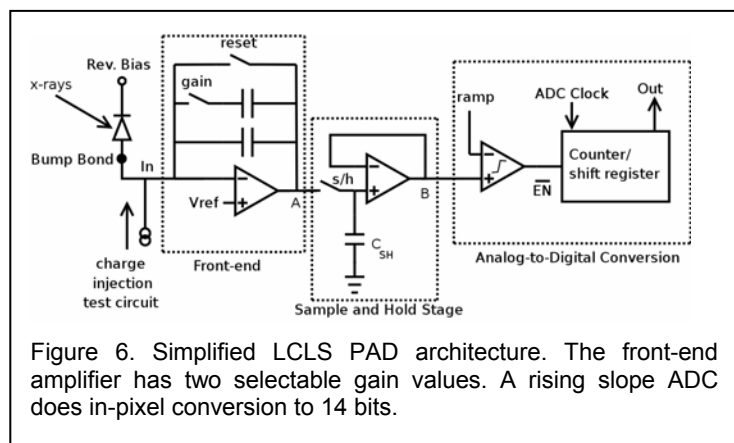
Figure 5. Diffraction from a large-grain Al foil. The same diffraction pattern is shown at increasing display magnification to illustrate the large dynamic range of the MMPAD. The ratio of intensities in the diffraction pattern are larger than  $10^5$ .

see Figure 5). The name Mixed-Mode PAD arises from the mixed analog-digital mode used.

A commercial variant of this design is being vended by ADSC. With additional DOE-BES and Keck Foundation support, we have built a 256 x 384 pixel detector that will be used for a series of x-ray microscopy and other imaging experiments at the Advanced Photon Source in Spring, 2012. The exceptionally wide dynamic range and fast framing of the MMPAD make it especially useful for coherent x-ray imaging and ptychography applications. The biological interest is primarily in using these methods to examine

nonperiodic biologically-derived materials. Recently, the MMPAD has been demonstrated as a quantum limited detector biomacromolecular solution scattering [32].

### 1.2.1.3 LCLS PAD



The LCLS PAD is designed to meet the stringent imaging requirements of the Coherent X-ray Imaging (CXI) experiment at the Linac Coherent Light Source (LCLS) being built at the Stanford Linear Accelerator Center (SLAC). The goal of CXI is to obtain macromolecular structures without crystals by exposing particles (such as proteins) one at a time to the LCLS beam. Each particle

lasts for only femtoseconds before it Coulomb explodes [33]. This places stringent specifications on the detector: The dynamic range of individual diffraction patterns range from about a few thousand x-rays/pix at low angles to far less than an average of 1 x-ray/pix at high angles. Photon counting architectures are precluded because the entire x-ray pattern arrives at the detector in femtoseconds, yet individual photons must be clearly distinguished well above the detector noise at high angles. The detector is also the data collecting instrument for the LCLS experiments to obtain macromolecular structures from proteins that are readily formed into nanocrystals, but not large crystals. It is believed that membrane proteins fall into this category.

Figure 6 shows a simplified pixel schematic of the PAD designed at Cornell [34-37]. A typical diffraction pattern has a well-defined envelope of intensity versus angle. At low angles, up to  $10^3$  x-rays/pix may be incident; at large angles, the average flux is  $< 1$  x-ray/pix. To accommodate this, a gain map is programmed into the detector such that regions with high flux have pixels with the lower gain and regions with low flux have a higher gain. Gains and the noise are such that all parts of the recorded pattern are completely dominated by the Poisson noise statistics of the incident image.

The Cornell LCLS PAD chips exceeded all required specifications. They are now built into the main detectors that have been installed in four out of the six LCLS stations, and are fundamental to an astounding number of science experiments that have just now started to appear in print.

### 1.2.1.4 Keck PAD

The Keck PAD (so named because primary support has come from a grant from the Keck Foundation) is a submicrosecond imager successor to the Prototype Microsecond Imager described in Section 1.2.1.1. The Keck PAD is in the middle of the development cycle. The pixel has been developed [34, 38] and a small 16 x 16 pixel imager has been built and tested [38, 39]. The small detector met all design specifications. The detector is capable of collecting up to 8 successive frames at rates of 150 ns/frame, with a well-

depth of about 4,000 8 keV x-rays/pix/frame, all with single x-ray sensitivity. It is designed to perform single bunch imaging experiments at, e.g., the Advanced Photon Source. Full scale 128 x 128 pixel imaging chips have been fabricated and are awaiting testing. If the large chips test well then a multi-module detector is expected to be operational in 2013.

#### **1.2.1.5 FPGA PAD**

The last PAD described in this Progress Report is at an early stage of development. It is primarily supported by DOE-BES and the Keck Foundation. The idea behind the FPGA PAD is to include a wide bandwidth pipeline to a resident Field Programmable Gate Array (FPGA). capable of performing, e.g., a time autocorrelation function operation in each pixel.

The beauty of this implementation is that the FPGA can be programmed to perform many different types of functions, effectively moving much of the specificity of the PAD from ASIC hardware to FPGA firmware. For example, one may consider an FPGA implementation to allow a 100 point time autocorrelation function to be online computed for each of the  $10^4$  pixels in the associated PAD chip, where each pixel can operate at up to  $10^6$  x-rays/pix/s. This implementation would allow X-ray Photon Correlation Spectroscopy (XPCS) experiments a time scales several orders of magnitude faster than now feasible. Alternatively, the same hardware can be reprogrammed (by modifying the FPGA firmware) to act as an x-ray lock-in amplifier, or in any one of a number of different specific detector applications. If the FPGA PAD is successful, it has promise to decrease the time and expense of developing new types of PADs.

A small scale fabrication of FPGA test ICs has been submitted. Testing of the ICs and development of the pixel is expected to proceed throughout 2012. The goal is to have a small working detector in 2013. As was the case for all the above mentioned PADs, infrastructural resources from the BER grant were critical to perform the initial development work.

### **1.3 High Pressure X-ray Crystallography**

The productivity of our group is a direct consequence of the philosophy of coupling instrumentation development with the performance of basic research. Over the years, this has led to innovations which are not confined to detector development, including humidity-control apparatus, solute-binding assays, muscle-tensioning equipment, beamline optics, time-resolved x-ray methods, image-intensified microscopy, and, most recently, methods to determine biomolecular structure at high pressures.

Much of the earth's life exists at high pressures (hi-P). Pressures encountered in ocean trenches reach 1.2 kbar. If bacterial life proves to be commonly present in deep sediments, as is increasingly thought to be the case [40], a significant fraction of life on earth may exist at pressures above 1 kbar. Moreover, understanding the details of

biomolecular machinery of microbes, and in particular, the piezophiles present in deep ocean trenches and vent systems, is a fundamental goal of the DOE-BER Genomes to Life (GTL) program. The question then arises: What are the effects of pressure on biological systems and how are these effects to be understood and utilized?

A second reason for study of the effects of pressure on biomolecular systems is that it provides insight on the detailed operation of biomolecular machinery. Pressure,  $P$ , and temperature,  $T$ , both contribute to the free energy of all biomolecular processes with opposite signs, e.g., as  $T\Delta S - P\Delta V$ , where  $S$  is the entropy and  $V$  is the volume. At first sight one might expect pressure effects to be small because proteins are very incompressible. However, this is misleading. Macromolecules have a very large number of conformational substates, many of which differ by very small free energies yet are the difference between a functionally active and an inactive molecule. In most biomolecular systems, the effect on the free energy of raising pressure by a kbar is comparable to lowering the temperature by many tens of degrees.

For this reason, pressures encountered in the biosphere have numerous and often very large effects on biomolecular systems, affecting kinetic and equilibrium constants, association of protein complexes and ligand binding, membrane permeability and ion transduction, cellular metabolism and morphology, viral infectivity, and protein folding [41-46]. (Numerous papers on pressure effects on biomolecular systems may be found in a special issue of *Biochem. Biophys. Acta* devoted to the subject [47]).

Pressure studies offer a novel method to engineer enzymes. Recent experiments in our laboratory [48-51] on a pressure-induced fluorescence shift in Citrine, a green fluorescent protein analog, have shown that the shift is a direct consequence of pressure-induced deformation of the enzyme. This deformation is the net result of many pressure-sensitive interactions in the protein, including changes in ionization and hydration of residues and volume reduction of tiny packing voids within the protein. Because the protein is a compact entity, deformations in one part of the protein tend to affect the relative position of neighboring residues throughout the protein. In the case of Citrine, the net effect is a bending of the overall  $\beta$ -barrel structure, which results in sub-Angstrom shifts of the relative positions of the two amino acids that form the fluorescent center, in turn resulting in the fluorescent shift. Knowing that bending of the  $\beta$ -barrel may induce the shift, one may envision mutating residues on opposite side of the  $\beta$ -barrel, introducing smaller residues on one side and bigger ones on the other, to induce a similar bend at room pressure. The expected result, yet to be verified, would be a fluorescent shift similar to the pressure-induced shift. This suggests a novel strategy to engineer Citrine: Suppose one wished to engineer Citrine to fluoresce at a different wavelength, say, one achieved at 2 kbar. Measure the structural deformation that gives rise to the shift. Then mutate specific residues in the protein to attempt to create a similar deformation. If the resultant deformation of the active site (e.g., the fluorescent center) is similar, the effect on the activity of the active site should also be similar.

This approach may be generalized. As noted earlier, the activity of many enzymes are pressure sensitive. As with Citrine, this is likely the result of global pressure-induced

deformation resulting in structural perturbations of active sites. The residues at active sites are precisely positioned such that average displacements of a few tenths of an angstrom may have large effects; indeed, the conformational changes at active sites upon catalysis are often only the scale of a few tenths of an angstrom. Suppose that it is observed that enzymatic function increases at a given pressure. The comparison of the detailed structure of the enzyme by crystallography, both at room and high pressure, indicates the specific type of active site deformation that is needed to increase enzyme function. This is important information for two reasons: First, it provides fundamental knowledge about the details of active sites. Second, it provides knowledge of how to change the structure of the active site so as to increase function. In some cases, this involves movement of, say, a given residue a few tenths of an angstrom in a given direction. In this case, it may be possible to mutate a small neighboring residue to a larger residue to induce a similar shift at the active site, hopefully resulting in higher activity.

The ability to perform this type of study is a direct consequence of the high pressure crystallographic and spectroscopic methods developed under this grant. Although a huge literature reports on observation of the effects of pressure on biomolecular machinery [47], with very rare exceptions a basic understanding of the effects is almost entirely absent. The lack of a molecular understanding of pressure effects stems directly from a dearth of studies on how pressure affects the structure of proteins and membranes. The reason for this paucity of data is the technical challenge of performing protein crystallography at kbar pressures. For example, prior to our work in 2002, the complete, high resolution structure of only one protein, lysozyme, had been solved at kbar pressures [52]!

Thanks to DOE-BER support, over the last decade our group has developed the technical tools to perform hi-P protein crystallography [53-58], hi-P Small Angle X-ray Scattering (SAXS) studies [59, 60], and hi-P optical characterization (e.g., fluorescence and optical absorption spectra) [51], and to make these tools available to the larger synchrotron user community. Two different hi-P crystallography methods have been developed: The first uses an x-ray transparent beryllium pressure vessel that can be mounted on a standard synchrotron crystallography goniometer [52, 57]. The second capitalizes on the observation that collective high pressure effects on tertiary structure may be frozen in by deep-cooling protein crystals to well below the glass transition temperature [61]. These techniques were applied to study myoglobin structure at pressures of up to 2 kbar [58]. Once frozen, the pressure may be released and the crystals examined by standard cryo-cooled crystallographic methods. We devised a numerical method to remove the elastic rebound that occurs when the deep-frozen crystals are released from pressure and showed that the collective pressure effects are, indeed, preserved [58]. More recent work has resulted in an apparatus to easily freeze crystals already mounted in a cryoloop in helium gas at up to 4 kbar, after which the crystals may be transferred at atmospheric pressure to a standard cryocooled crystallography station [53-56, 62, 63]. This method has proven to yield superior diffraction for crystals that are difficult to cryocool. It also enables stabilization of ligands

and substrates in crystals, a feature that turned out to be critical for studies of an important membrane protein complex [64].

As a result of this work, it is now possible to routinely examine pressure effects on a wide variety of protein systems. Recent results have provided important insight into some of the most fundamental questions of proteins. For example, in 1914 Bridgman showed that proteins unfold under pressure, but the mechanism of unfolding, and similarities to thermal or chemical denaturation, have been hotly debated [65]. Using Hi-P crystallographic studies of T4 lysozyme we have been able to show that unfolding is driven by internal hydration of cavities, and that these cavities hydrate even if they are highly hydrophobic [66-68]. Most recently, we have used hi-P spectroscopy and SAXS to show that the hydration of internal cavities drives a progressive unraveling of tertiary structure, leaving a partially denatured protein [69], consistent with earlier studies on *Staphylococcal* nuclease [65]. These studies beg the issue of what hydrophobicity means as a driving potential for the folding of proteins. And, as mentioned above, high-pressure crystallography and spectroscopy have reveals the mechanism of the fluorescence shift in Citrine.

The work described above opens a host of important questions for the future: What rearrangements of tertiary structure occur with pressure? Our observations so far on a half dozen proteins suggest that the rearrangements are small but functionally significant. Can the changes in particular regions of a protein be understood in terms of the specific residues in that part of the structure, or are the changes more related to collective effects? What changes occur in the protein contact regions in multimeric complexes? What is the extent and role of water penetration into hydrophobic domains? What structural rearrangements under pressure lead to changes in ligand binding at specific binding sites? Can we combine information from crystallographic fluctuation analysis and solution scattering to identify the parts of the protein that unfold first and then understand this in terms of the residues involved? Can this information be use to engineer specific properties into enzymes?

The high pressure studies supported by the DOE-BER grant were recently summarized in an invited review on high pressure effects on biomacromolecules [70].

## **1.4 Novel Mesophase Materials Derived from Block Co-polymers**

The detectors and technology developed under this DOE-BER grant also contribute to a variety of experiments in materials science and energy technology. The primary emphasis recently has been on the development of novel complex composite materials whose structural form is dictated by the self-assembly of block copolymer mesophases. These materials are being studied for applications in battery electrodes, solar cells, and biosensors. These materials and applications are highly diverse. For this reason, the work will not be described here, save to say that the work is has been very influential and ground breaking. Specific references are [71-94]. A measure of the influence of these papers is that they have been cited about 700 times to date.

## 1.5 Publications Since Prior Progress Report

### Papers (20)

1. Sol M. Gruner (2010). Synchrotron area detectors, present and future. Plenary paper presented at SRI09, Melbourne, Australia, 27 Sept - 2 Oct, 2009. AIP Conf. Proceedings 1234 : 69-72. <http://link.aip.org/link/?APCPCS/1234/69/1>
2. Teeraporn Suteewong, Hiroaki Sai, Jinwoo Lee, Taeghwan Hyeon, Sol M. Gruner and Ulrich Wiesner (2010). Ordered Mesoporous Silica Nanoparticles with and without Embedded Iron Oxide Nanoparticles: Structure Evolution during Synthesis. *J. Materials Chem.* 20 : 7807-7814.
3. Lucas J. Koerner & Sol M. Gruner (2011). X-ray analog pixel array detector for single bunch time-resolved imaging. *J. Synchrotron Rad.* 18 : 157-164. doi:10.1107/S090904951004104X.
4. Lucas J. Koerner, Richard E. Gillilan, Katharine S. Green, Suntao Wang, Sol M. Gruner (2011). Small angle solution scattering using the mixed-mode pixel array detector. *J. Synchrotron Rad.* 18 : 148-156. doi:10.1107/S0909049510045607.
5. Teeraporn Suteewong, Hiroaki Sai, Roy Cohen, Suntao Wang, Michelle Bradbury, Barbara Baird, Sol Gruner, Ulrich Wiesner (2011). Highly aminated mesoporous silica nanoparticles with cubic pore structure. *J. Amer. Chem. Soc.* 133 : 172-175. doi:10.1021/ja1061664
6. Hugh T. Philipp, Marianne Hromalik, Mark Tate, Lucas Koerner, Sol M. Gruner (2011). Pixel array detector for x-ray free electron laser experiments. *Nuclear Instruments and Methods in Physics Research A* 649 : 67-69. doi:10.1016/j.nima.2010.11.189.
7. Morgan Stefik, Syrbhi Mahajan, Hiroaki Sai, Thomas H. Epps III, Frank S. Bates, Sol M. Gruner, Ulrich Wiesner (2010). Networked nanocomposites derived from block terpolymers. *Abstr of Papers of the ACS, Aug 2010, San Francisco, CA. In PMSE Preprints (2010).*
8. Stephen T. Kelly, Jonathan C. Trenkle, Lucas J. Koerner, Sara C. Barron, Noel Walker, Philippe O. Pouliquen, Mark W. Tate, Sol M. Gruner, Eric M. Dufresne, Timothy P. Weihs and Todd C. Hufnagel (2011). Fast x-ray microdiffraction techniques for studying irreversible transformations in materials. *J. Synchrotron Radiation* 18: 464-474.

9. Marcus D. Collins, Chae Un Kim, Sol M. Gruner (2011). High-Pressure Protein Crystallography and NMR to Explore Protein Conformations. *Annu. Rev. Biophys.* 40: 81-98.
10. Hugh T. Philipp, Mark W. Tate, Sol M. Gruner (2011). Low-flux measurements with Cornell's LCLS integrating pixel array detector. *J. Instrumentation* 6 : C11006. (<http://iopscience.iop.org/1748-0221/6/11/C11006>).
11. Chae Un Kim, Mark W. Tate, and Sol M. Gruner (2011). Protein Dynamical Transition at 110 K. *Proceed. Natl. Acad. Sci, USA.* 108 : 20897-20901.
12. Morgan Stefik, Suntao Wang, Robert Hovden, Hiroaki Sai, Mark Tate, David Muller, Ullrich Steiner, Sol Gruner, Ulrich Wiesner (2012). Networked and chiral nanocomposites from ABC triblock terpolymer coassembly with transition metal oxide nanoparticles. *J. Materials Chem.* 22: 1078 – 1087.
13. Darren Dale, Sol M. Gruner, Joel Brock, Don Bilderback, Ernie Fontes (2011). Science at the hard x-ray diffraction limit (XDL2011), Part I. *Synchrotron Radiation News* 24 : 4- 12.
14. Suntao Wang, Mark Tate, Sol M. Gruner. Protein crowding impedes pressure-induced unfolding of staphylococcal nuclease. (Submitted for publication)
15. Suntao Wang, Yu-fei Meng, Nozomi Ando, Mark Tate, Szczesny Krasnicki, Chih-shiue Yan, Qi Liang, Joseph Lai, Ho-kwang Mao, Sol M. Gruner and Russell J. Hemley. Single-crystal CVD diamonds as small-angle X-ray scattering windows for high pressure research. (Submitted for publication)
16. Teeraporn Suteewong, Hiroaki Sai, Michelle Bradbury, Lara A. Estroff, Sol M. Gruner and Ulrich Wiesner. Synthesis and Formation Mechanism of Aminated Mesoporous Silica Nanoparticles. (Submitted for publication)
17. Hugh T. Philipp, Kartik Ayyer, Mark W. Tate, Veit Elser, Sol M. Gruner. Reconstruction of X-ray Intensity from Extremely Low-Flux Images of Randomly Oriented Samples. (Submitted for publication)
18. Sebastien Boutet et al. High resolution protein structure determination by serial femtosecond crystallography. (Submitted for publication)
19. Eric R. Meshot, Eric A. Verploegen, Mostafa Bedewy, Sameh Tawfick, Arthur R. Woll, Kate Green, Marianne Hromalik, Lucas J. Koerner, Hugh Philipp, Mark W. Tate, Sol M. Gruner, and A. John Hart. Rapid dynamics of catalyst film dewetting and carbon nanotube self-organization revealed by *in situ* X-ray scattering. (Submitted for publication)

## Theses (1)

1. Yi-Fan Chen (2012). Phase behavior of cardiolipin. (Cornell University, Field of Biophysics).

## Abstracts and Presentations (4)

1. H. T. Philipp, M. Hromalik, M. Tate, L. Koerner, and S. M. Gruner (2010). Pixel Array Detector for X-ray Free-Electron Laser Experiments. The 16<sup>th</sup> Pan-American Synchrotron Radiation Instrumentation Conference, Argonne National Laboratory, Sept. 21-24, 2010.
2. C. U. Kim, S. M. Gruner (2010). High Pressure Study on Water inside Protein Crystals. IUCr Commission on High Pressure 2010, Park Vista, Gatlinburg, TN, Sept. 19 – 23, 2010.
3. R. M. Baur, D. S. Dale, L. Assoufid, X. Xiao, A. T. Macrander, S. Rutishauser, C. Davi, S. M. Gruner (2010). Development of a Talbot interferometer at the CHESS F3 beamline. The 10<sup>th</sup> International Conf. On X-ray Microscopy, Argonne National Laboratory, July 15 – Sept. 15, 2010.
4. H. Philipp, M. Tate, S. Gruner (2011). Single-Photon Thresholding for Low-flux Measurements in Charge-Integrating Pixel Array Detectors. International Workshop on Radiation Imaging Detectors iWoRID, Zurich, Switzerland, July 3 – 7, 2011.

## 1.6 References

1. Gruner, S.M., *Synchrotron Radiation and Detectors: Synergists in a Dance*. Transactions ACA, 1999. **34**: p. 11-25.
2. Gruner, S.M., M.W. Tate, and E.F. Eikenberry, *Charge-coupled device area x-ray detectors*. Rev. of Scientific Instruments, 2002. **73**(8): p. 2815.
3. Gruner, S.M., *Stability of Lyotropic Phases with Curved Interfaces*. J. Phys. Chem., 1989. **93**(22): p. 7562-7570.
4. Anderson, D., S.M. Gruner, and S. Leibler, *Geometrical Aspects of the Frustration In The Cubic Phases of Lyotropic Liquid Crystals*. Proc. Natl. Acad. Sci., 1988. **85**: p. 5364-5368.
5. Gruner, S.M., *Intrinsic curvature hypothesis for biomembrane lipid composition: A Role for non-bilayer lipids*. Proc. Natl. Acad. Sci. USA, 1985. **82**: p. 3665-3669.
6. So, P.T.C., *PhD thesis: High pressure effects on the mesophases of lipid-water systems*, in *Physics*. 1992, Princeton University: Princeton, NJ.

7. Hajduk, D.A., *PhD thesis: Morphological Transitions in Block Copolymers*, in *Physics*. 1994, Princeton University: Princeton, NJ.
8. Fernandez, P. *SRI 2005 Detector Workshop Summary*. [http://www.aps.anl.gov/News/Meetings/Monthly\\_Meetings/2005/Presentations/20051214\\_PFernandez.pdf](http://www.aps.anl.gov/News/Meetings/Monthly_Meetings/2005/Presentations/20051214_PFernandez.pdf). in *SRI 2005 Detector Workshop*. 2005. Advanced Photon Source, Argonne National Laboratory, Argonne, IL.
9. Thompson, A., et.al, *A Program in Detector Development for the US Synchrotron Radiation Community.*, in <http://www-esg.lbl.gov/Conferences%20&%20Meetings/detectorsync/DetectorSyncWhitePaper0801.pdf>. 2000: Washington, D.C.
10. Graafsma, H., *Introduction to the special issue on detectors*. *Journal of Synchrotron Radiation*, 2006. **13**: p. 97-98.
11. Graafsma, H. and O. Peyret, *Proceedings of the 7th International Workshop on Radiation Imaging Detectors - ESRF, Grenoble, France, July 4-7, 2005*. Nuclear Instruments & Methods in Physics Research Section a-Accelerators Spectrometers Detectors and Associated Equipment, 2006. **563**(1): p. Vii-Vii.
12. Gruner, S., Mills, D., Thompson, A., *Detector Workshop Proposes Coordinated Detector Development for Synchrotron Facilities*. 2006. **19**(3).
13. Barna, S.L., *Development of a microsecond framing two-dimensional pixel array detector (PAD) for time-resolved x-ray diffraction.*, in *Physics Dept*. 1996, Princeton University: Princeton, NJ.
14. Barna, S.L., Shepherd, J.A., Wixted, R.L., Tate, M.W., Rodricks, B., Gruner, S.M., *Development of a fast pixel array detector for use in microsecond time-resolved x-ray diffraction*. *Proc. SPIE*, 1995. **2521**: p. 301-309.
15. Barna, S.L., Shepherd, J.A., Tate, M.W., Wixted, R.L., Eikenberry, E.F., Gruner, S.M., *Characterization of Prototype Pixel Array Detector (PAD) for Use in Microsecond Framing Time-Resolved X-Ray Diffraction Studies*. *IEEE Trans. Nucl. Sci.*, 1997. **44**(3): p. 950-956.
16. Eikenberry, E.F., Barna, S.L., Tate, M.W., Rossi, G., Wixted, R.L., Sellin, P.J., Gruner, S.M., *A Pixel-Array Detector for Time-Resolved X-ray Diffraction*. *J. Synchrotron Rad.*, 1998. **5**: p. 252-255.
17. Rossi, G., Renzi, M., Eikenberry, E.F., Tate, M.W., Bilderback, D., Fontes, E., Wixted, R., Barna, S., Gruner, S.M., *Tests of a prototype pixel array detector for microsecond time-resolved X-ray diffraction*. *J. Synchrotron Rad.*, 1999. **6**: p. 1096-1105.
18. Rossi, G., Renzi, M.J., Eikenberry, E.F., Tate, M.W., Bilderback, D., Fontes, E., Wixted, R., Barna, S., Gruner, S.M., *Development of Pixel Array Detector for Time Resolved X-ray Imaging*. *Synchrotron Radiation Instrumentation: Eleventh US National Conference*, 2000: p. 311-316.
19. Sellin, P.J., Rossi, G., Renzi, M.J., Knights, A.P., Eikenberry, E.F., Tate, M.W., Barna, S.L., Wixted, R.L., Gruner, S.M., *Performance of semi-insulating gallium*

- arsenide X-ray pixel detectors with current-integrating readout*. Nuclear Instruments and Methods in Physics Research A, 2001. **460**: p. 207-212.
20. Cai, W., Powell, C.F., Yue, Y., Narayanan, S., Wang, J., Tate, M.W., Renzi, M.J., Ercan, A., Fontes, E., Gruner, S.M., *Quantitative analysis of highly transient fuel sprays by time-resolved x-radiography*. Appl. Phys. Lett., 2003. **83**(8): p. 1671.
  21. Ercan, A., Tate, M.W., Gruner, S.M., *Analog pixel array detectors*. Journal of Synchrotron Radiation, 2006. **13**: p. 110-119.
  22. Liu, X., Im, K. S., Wang, Y., Wang, J., Hung, D. L. S., Winkelman, J. R., Tate, M. W., Ercan, A., Koerner, L.J., Caswell, T., Chamberlain, D., Schuette, D. R., Philipp, H., Smilgies, D. M., Gruner, S. M., *Quantitative Characterization of Near-Field Fuel Sprays by Multi-Orifice Direct Injection Using Ultrafast X-Tomography Technique*. SAE 2006 Transactions: Journal of Engines, 2006. **Society of Automotive Engineers Technical Paper 2006-01-1041**.
  23. Liu, X., Liu, J., Li, X., Cheong, S-K., Shy, D., Wang, J., Tate, M.W., Ercan, A., Schuette, D.R., Renzi, M.J., Woll, A., Gruner, S.M., *Development of ultrafast computed tomography of highly transient fuel sprays*. Proc. SPIE, 2004. **5535**: p. 21-28.
  24. MacPhee, A.G., Tate, M.W., Powell, C.F., Yue, Y., Renzi, M.J., Ercan, A., Narayanan, S., Fontes, E., Walther, J., Schaller, J., Gruner, S.M., Wang, J., *X-ray Imaging of Shock Waves Generated by High-Pressure Fuel Sprays*. Science, 2002. **295**: p. 1261.
  25. Trenkle, J.C., Koerner, L., Gruner, S., Weihs, T. P., Hufnagel, T. C., *In-situ x-ray diffraction of phase transformations in a nanostructured reactive multilayer foils (Abstract)*. Fifth International conference on Synchrotron Radiation in Materials Science July 30-August 2, 2006, Chicago, Illinois, 2006.
  26. Kelly, S.T., et al., *Fast X-ray microdiffraction techniques for studying irreversible transformations in materials*. Journal of Synchrotron Radiation, 2011. **18**: p. 464-474.
  27. Trenkle, J.C., et al., *Time-resolved x-ray microdiffraction studies of phase transformations during rapidly propagating reactions in Al/Ni and Zr/Ni multilayer foils*. Journal of Applied Physics, 2010. **107**(11).
  28. Angello, A.G., Augusting, F., Ecan, A., Gruner, S., Hamlin, R., Hontz, T., Renzi, M., Schuette, D., Tate, M., Vernon, W., *Development of a mixed-mode pixel array detector for macromolecular crystallography*. Nuclear Science Symposium Conference Record, 2004. **IEEE 7**: p. 4667 - 4671.
  29. Vernon, W., Allin, M., Hamlin, R., Hontz, T., Nguyen, D., Augustine, F., Gruner, S. M., Xuong, Ng H., Schuette, D. R., Tate, M. W., Koerner, L. J. *First results from the 128x128 pixel mixed-mode Si x-ray detector chip (abstract)*. in *Hard X-Ray and Gamma-Ray Detector Physics IX*. 2007. San Diego, CA, USA: SPIE.
  30. Renzi, M.J., *Pixel Array Detectors for Ultra-Fast Time-Resolved X-ray Imaging*. PhD Thesis, Dept. of Applied & Engineering Physics (Cornell), 2003.

31. Schuette, D.R., *PhD Thesis: A mixed analog and digital pixel array detector for synchrotron x-ray imaging.*, in *Physics*. 2008, Cornell University: Ithaca, NY.
32. Koerner, L.J., et al., *Small-angle solution scattering using the mixed-mode pixel array detector*. *Journal of Synchrotron Radiation*, 2011. **18**: p. 148-156.
33. Neutze, R., Wouts, R., van der Spoel, D., Weckert, E., Hajdu, J., *Potential for biomolecular imaging with femtosecond X-ray pulses*. *Nature*, 2000. **406**: p. 752.
34. Koerner, L.J., et al., *X-ray tests of a Pixel Array Detector for coherent x-ray imaging at the Linac Coherent Light Source*. *Journal of Instrumentation*, 2009. **4**.
35. Philipp, H.T., et al., *Pixel array detector for X-ray free electron laser experiments*. *Nuclear Instruments & Methods in Physics Research Section a-Accelerators Spectrometers Detectors and Associated Equipment*, 2011. **649**(1): p. 67-69.
36. Philipp, H.T., et al., *Femtosecond Radiation Experiment Detector for X-Ray Free-Electron Laser (XFEL) Coherent X-Ray Imaging*. *IEEE Transactions on Nuclear Science*, 2010. **57**(6): p. 3795-3799.
37. Philipp, H.T., M.W. Tate, and S.M. Gruner, *Low-flux measurements with Cornell's LCLS integrating pixel array detector*. *Journal of Instrumentation*, 2011. **6**.
38. Koerner, L.J., *PhD Thesis: X-ray analog pixel array detector for single synchrotron bunch time-resolved imaging*, in *Physics*. 2010, Cornell University: Ithaca, NY.
39. Koerner, L.J. and S.M. Gruner, *X-ray analog pixel array detector for single synchrotron bunch time-resolved imaging*. *Journal of Synchrotron Radiation*, 2011. **18**: p. 157-164.
40. Stevens, T.O., McKinley, J.P., *Lithoautotrophic microbial ecosystems in deep basalt aquifers*. *Science (Washington, D. C., 1883-)*, 1995. **270**: p. 450-454.
41. Heremans, K., *High pressure effects on proteins and other biomolecules*. *Ann. Rev. Biophys. Bioeng.*, 1982. **11**: p. 1-21.
42. Silva, J.L., Weber, G., *Pressure stability of proteins*. *Annu. Rev. Phys. Chem.*, 1993. **44**: p. 89-113.
43. Jonas, J., Jonas A., *High-pressure NMR spectroscopy of proteins and membranes*. *Annu. Rev. Biophys. Biomol. Struct.*, 1994. **23**: p. 287-318.
44. Gross, M., Jaenicke, R., *Proteins under pressure*. *Eur. J. Biochem.*, 1994. **221**: p. 617-630.
45. Bartlett, D.H., Kato, C. and Horikoshi, K., *High pressure influences on gene and protein expression*. *Res. Microbiol.*, 1995. **146**: p. 697-706.
46. Mozhaev, V.V., Heremans, K., Frank, J., Masson, P., Balny, C., *High pressure effects on protein structure and function*. *Proteins: Structure, Function, and Genetics*, 1996. **24**: p. 81-91.
47. Ernst, R.R., *Preface (to a special issue of BBA on the effects of pressure on living machinery)*. *Biochimica Et Biophysica Acta*, 2002. **1595**: p. 1-2.

48. Barstow, B., Ando, N., Kim, C. U., D'Acchioli, J. D., Gruner, S. M. *The Structural Basis of a Fluorescence Red Shift of Citrine Under Pressure (abstract & poster)*. in *CHESS Users Meeting*. 2006. Ithaca, NY, 13 June 2006.
49. Barstow, B., Ando, N., Kim, C., Gruner, S. M. *The Fluorescence Red Shift of Citrine Under High Pressure*. in *Biophys. Soc. Annual Meeting*. 2007. Baltimore, MD 3-7 Mar., 2007.
50. Barstow, B., et al., *Coupling of Pressure-Induced Structural Shifts to Spectral Changes in a Yellow Fluorescent Protein*. *Biophysical Journal*, 2009. **97**(6): p. 1719-1727.
51. Barstow, B., Ando, N., Kim, C. U., Gruner, S. M., *Alteration of Citrine Structure by Hydrostatic Pressure Explains the Accompanying Spectral Shift*. Submitted to *Proc. Natl. Acad. Sci. USA*, 2008.
52. Kundrot, C.E., Richards, F.M., *Crystal structure of hen egg-white lysozyme at a hydrostatic pressure of 1000 atmospheres*. *J. Mol. Biol.*, 1987. **193**: p. 157-170.
53. Kim, C.U., Kapfer, R., Gruner, S. M., *High-pressure cooling of protein crystals without cryoprotectants*. *Acta Crystallographica Section D-Biological Crystallography*, 2005. **61**: p. 881-890.
54. Kim, C.U., Hao, Q., Gruner, S. M., *High-pressure cryocooling for capillary sample cryoprotection and diffraction phasing at long wavelengths*. *Acta Crystallographica Section D-Biological Crystallography*, 2007. **63**: p. 653-659.
55. Kim, C.U., Chen, Y-F., Tate, M.W., Gruner, S.M., *Pressure-induced high-density amorphous ice in protein crystals*. *J. Appl. Cryst.*, 2008. **41**: p. 1-7.
56. Kim, C.U., Q. Hao, and S.M. Gruner, *Solution of protein crystallographic structures by high-pressure cryocooling and noble-gas phasing*. *Acta Crystallographica Section D-Biological Crystallography*, 2006. **62**: p. 687-694.
57. Urayama, P., *Techniques for high pressure macromolecular crystallography and the effects of pressure on the structure of sperm whale myoglobin*, in *Physics*. 2001, Princeton University: Princeton, NJ.
58. Urayama, P., Phillips Jr., G.N., Gruner, S.M., *Probing Substates in Sperm Whale Myoglobin Using High-Pressure Crystallography*. *Structure*, 2002. **10**: p. 51-60.
59. Ando, N., Chenevier, P., Gruner, S.M. *A new high pressure SAXS cell for protein denaturation studies on microvolumes (abstract)*. in *15th IUPAB & 5th EBSA International Biophysics Congress 2005*. 2005. Montpellier, France, 27 Aug. - 1 Sept., 2005.
60. Ando, N., Chenevier, P., Novak, M., Tate, M. W., Gruner, S. M., *High hydrostatic pressure small-angle X-ray scattering cell for protein solution studies featuring diamond windows and disposable sample cells*. *J. of Appl. Crystallography*, 2008. **41**: p. 167-175.
61. Thomanek, U.F., Parak, F., Mössbauer, R. L., Formanek, H., Schwager, P., Hoppe, W., *Freezing of myoglobin crystals at high pressure*. *Acta Cryst.*, 1973. **A29**: p. 263-265.

62. Kim, C.U., et al., *Evidence for liquid water during the high-density to low-density amorphous ice transition*. Proceedings of the National Academy of Sciences of the United States of America, 2009. **106**(12): p. 4596-4600.
63. Kim, C.U., M.W. Tate, and S.M. Gruner, *Protein dynamical transition at 110 K*. Proceedings of the National Academy of Sciences of the United States of America, 2011. **108**(52): p. 20897-20901.
64. Albright, R.A., et al., *The RCK domain of the KtrAB K<sup>+</sup> transporter: Multiple conformations of an octameric ring*. Cell, 2006. **126**(6): p. 1147-1159.
65. Paliwal, A., Asthagiri, D., Bossev, D. P., Paulaitis, M. E., *Pressure Denaturation of Staphylococcal Nuclease Studied by Neutron Small-Angle Scattering and Molecular Simulation*. Biophysical Journal, 2004. **87**: p. 3479-3492.
66. Collins, M.D., Quillin, M. L., Hummer, G., Matthews, B. W., Gruner, S. M., *Structural Rigidity of a Large Cavity-containing Protein Revealed by High-pressure Crystallography*. J. Mol. Biol., 2007. **367**: p. 752-763.
67. Collins, M.D., *High-Pressure X-ray Crystallography and Core Hydrophobicity of T4 Lysozymes*, in *Ph.D. in Physics Dept.* 2006, Cornell University: Ithaca, NY.
68. Collins, M.D., Hummer, G., Quillin, M. L., Matthews, B. W., Gruner, S. M., *Cooperative water filling of a nonpolar protein cavity observed by high-pressure crystallography and simulation*. PNAS, 2005. **102**(45): p. 16668-16671.
69. Ando, N., Barstow, B., Baase, W.A., Fields, A., Matthews, B.W., Gruner, S.M., *The contribution of internal cavities to the thermodynamic stability of T4 Lysozyme mutants as a function of pressure*. To be submitted to Biochem., 2008.
70. Collins, M.D., C.U. Kim, and S.M. Gruner, *High-Pressure Protein Crystallography and NMR to Explore Protein Conformations*, in *Annual Review of Biophysics, Vol 40*, D.C. Rees, K.A. Dill, and J.R. Williamson, Editors. 2011. p. 81-98.
71. Cho, B.K., Jain, A., Gruner, S. M., Wiesner, U., *Mesophase Structure-Mechanical and Ionic Transport Correlations in Extended Amphiphilic Dendrons*. Science, 2004a. **305**: p. 1598.
72. Cho, B.K., Jain, A., Nieberle, J., Mahajan, S., Wiesner, U., Gruner, S., Turk, S., Rader, H. J., *Synthesis and Self-Assembly of Amphiphilic Dendrimers Based on Aliphatic Polyether-Type Dendritic Cores*. Macromolecules, 2004b. **37**: p. 4227-4234.
73. Cho, B.K., Jain, A., Gruner, S. M., Wiesner, U., *Nanoparticle-Induced Packing Transition in Mesosstructured Block Dendron-Silica Hybrids*. Chem. Mater., 2007. **19**: p. 3611-3614.
74. Du, P., Li, M., Douki, K., Li, X., Garcia, C. B. W., Jain, A., Smilgies, D. M., Fetters, L. J., Gruner, S. M., Wiesner, U., Ober, C. K., *Additive-Driven Phase-Selective Chemistry in Block Copolymer Thin Films: The Convergence of Top-Down and Bottom-Up Approaches*. Advanced Material, 2004. **16**(12): p. 953.
75. Finnefrock, A.C., Ulrich, R., Du Chesne, A., Honeker, C.C., Schumacher, K., Unger, K.K., Gruner, S.M., Wiesner, U., *Metal Oxide Containing Mesoporous*

- Silica with Bicontinuous 'Plumber's Nightmare' Morphology from a Block Copolymer - Hybrid Mesophase*. *Angew. Chem. Int. Ed.*, 2001. **40**(7): p. 1207-1211.
76. Finnefrock, A.C., Ulrich, R., Toombes, G. E. S., Gruner, S. M., Wiesner, U., *The Plumber's Nightmare: A New Morphology in Block Copolymer-Ceramic Nanocomposites and Mesoporous Aluminosilicates*. *J. Am. Chem. Soc.*, 2003. **125**(43): p. 13084-13093.
  77. Garcia, B.C., et al., *Morphology Diagram of a Diblock Copolymer-Aluminosilicate Nanoparticle System*. *Chemistry of Materials*, 2009. **21**(22): p. 5397-5405.
  78. Jain, A., Gutmann, J.S., Garcia, C.B.W., Zhang, Y., Tate, M.W., Gruner, S.M., Wiesner, U., *Effect of Filler Dimensionality on the Order-Disorder Transition of a Model Block Copolymer Nanocomposite*. *Macromolecules*, 2002. **35**: p. 4862-4865.
  79. Jain, A., Toombes, G. E. S., Hall, L. M., Mahajan, S., Garcia, C. B. W., Probst, W., Gruner, S. M., Wiesner, U., *Direct Access to Bicontinuous Skeletal Inorganic Plumber's Nightmare Networks from Block Copolymers*. *Angew. Chem. Int. Ed.*, 2005. **44**: p. 1226-1229.
  80. Jain, A., Hall, L. M., Garcia, C. B. W., Gruner, S. M., Wiesner, U., *Flow-Induced Alignment of Block Copolymer-Sol Nanoparticle Coassemblies toward Oriented Bulk Polymer-Silica Hybrids*. *Macromolecules*, 2005. **38**: p. 10095-10100.
  81. Kamperman, M., et al., *Integrating Structure Control over Multiple Length Scales in Porous High Temperature Ceramics with Functional Platinum Nanoparticles*. *Nano Letters*, 2009. **9**(7): p. 2756-2762.
  82. Li, Z.H., et al., *Metal Nanoparticle-Block Copolymer Composite Assembly and Disassembly*. *Chemistry of Materials*, 2009. **21**(23): p. 5578-5584.
  83. Mahajan, S., Renker, S., Simon, P. F. W., Gutmann, J. S., Jain, A., Gruner, S. M., Fetters, L. J., Coates, G. W., Wiesner, U., *Synthesis and Characterization of Amphiphilic Poly (ethylene oxide)-block-poly (hexyl methacrylate) Copolymers*. *Macromolecular Chemistry and Physics*, 2003. **204**: p. 1047-1055.
  84. Renker, S., Mahajan, S., Babski, D. T., Schnell, I., Jain, A., Gutmann, J., Zhang, Y., Gruner, S. M., Spiess, H. W., Wiesner, U., *Nanostructure and Shape Control in Polymer-Ceramic Hybrids from Poly (ethylene oxide)-block-Poly (hexyl methacrylate) and Aluminosilicates Derived from Them*. *Macromolecular Chemistry and Physics*, 2004. **205**: p. 1021-1030.
  85. Stefik, M., et al., *Ordered Three- and Five-ply Nanocomposites from ABC Block Terpolymer Microphase Separation with Niobia and Aluminosilicate Sols*. *Chemistry of Materials*, 2009. **21**(22): p. 5466-5473.
  86. Stefik, M., et al., *Three-Component Porous-Carbon-Titania Nanocomposites through Self-Assembly of ABCBA Block Terpolymers with Titania Sols*. *Macromolecules*, 2009. **42**(17): p. 6682-6687.

87. Suteewong, T., et al., *Highly Aminated Mesoporous Silica Nanoparticles with Cubic Pore Structure*. Journal of the American Chemical Society, 2011. **133**(2): p. 172-175.
88. Suteewong, T., et al., *Ordered mesoporous silica nanoparticles with and without embedded iron oxide nanoparticles: structure evolution during synthesis*. Journal of Materials Chemistry, 2010. **20**(36): p. 7807-7814.
89. Templin, M., Franck, A., Du Chesene, A., Leist, H., Zhang, Y., Ulrich, R., Schadler, V., Wiesner, U., *Organically Modified Aluminosilicate Mesostructures from Block Copolymer Phases*. Science, 1997. **278**: p. 1795-1798.
90. Toombes, G.E.S., et al., *A re-evaluation of the morphology of a bicontinuous block copolymer-ceramic material*. Macromolecules, 2007. **40**(25): p. 8974-8982.
91. Toombes, G.E.S., et al., *Hexagonally patterned lamellar morphology in ABC triblock copolymer/aluminosilicate nanocomposites*. Chemistry of Materials, 2008. **20**(10): p. 3278-3287.
92. Toombes, G.E.S., et al., *Self-assembly of four-layer woodpile structure from zigzag ABC copolymer/aluminosilicate concertinas*. Macromolecules, 2008. **41**(3): p. 852-859.
93. Ulrich, R., Finnefrock, A. C., Du Chesne, A., Mahajan, S., Simon, P. F. W., Gruner, S. M., Wiesner, U., *Polymer Ceramic Interfaces Through Self Assembly of Block Copolymers*. Polymeric Materials: Science & Engineering, 2001. **84**.
94. Warren, S.C., et al., *Ordered mesoporous materials from metal nanoparticle-block copolymer self-assembly*. Science, 2008. **320**(5884): p. 1748-1752.